Annals of Work Exposures and Health, 2019, 1–10
doi: 10.1093/annweh/wxy101
Original Article

Original Article

Relative Differences in Concentration Levels during Sawing and Drilling of Car Bumpers Containing MWCNT and Organic Pigment

Eelco Kuijpers[1,2*], Anjoeka Pronk[1], Antti Joonas Koivisto[3], Keld Alstrup Jensen[3], Roel Vermeulen[2] and Wouter Fransman[1]

[1]TNO, Utrechtseweg 48, 3704 HE Zeist, PO Box 360, The Netherlands; [2]Division of Environmental Epidemiology, Institute for Risk Assessment Sciences, Utrecht University, Yalelaan 2, 3584 CM Utrecht, The Netherlands; [3]National Research Centre for the Working Environment, Lerso Parkallé 105, DK-2100 Copenhagen, Denmark

*Author to whom correspondence should be addressed. e-mail: eelco.kuijpers@tno.nl

Submitted 11 July 2018; revised 24 October 2018; editorial decision 3 November 2018; revised version accepted 27 November 2018.

Abstract

Introduction: Knowledge on the exposure characteristics, including release of nanomaterials, is especially needed in the later stages of nano-enabled products' life cycles to perform better occupational risk assessments. The objective of this study was to assess the concentrations during sawing and drilling in car bumpers containing multi-walled carbon nanotubes (MWCNTs) and nanosized organic pigment (OP) under variable realistic workplace situations related to the ventilation in the room and machine settings.

Methods: Twelve different experiments were performed in triplicate ($N = 36$) using tools powered by induction engines that allow interference-free particle measurements. A DiSCmini was used to measure particle number concentrations, whereas particle size distributions were measured using Aerodynamic Particle Sizer (TSI), Scanning Mobility Particle Sizer (TSI), and Electrical Low Pressure Impactor (Dekati). In addition, inhalable particles were sampled using IOM samplers on filters for scanning electron microscope/energy-dispersive X-ray spectrometry (SEM/EDX) analyses. Data were analysed to estimate the effects of individual exposure determinants, in a two-stage modelling strategy using Autoregressive Integrated Moving Average models (stage 1) and subsequently combining first stage results in simulations using multiple linear regression models (stage 2).

Results: In sawing experiments, partly melted carbon-rich particles (mainly ~2 to ~8 μm) were identified with SEM/EDX, whereas drilling experiments revealed no activity-related particles. In addition, no pristine engineered nanoparticles (MWCNTs and OP) were observed to be liberated from the matrix. Statistical analyses showed significant effects of a higher sawing speed, a reduction in air concentration due to mechanical ventilation, and less exposure during sawing of car bumpers containing MWCNTs compared to bumpers containing OP.

Conclusion: The experiments in this study give an indication of the effects of different abrasive activities (sawing, drilling), machine settings (sawing speed, drill size), mechanical ventilation, and material characteristics on the manufactured nano-objects, their agglomerates, and aggregates concentration levels.

Keywords: abrasion; drilling; nanomaterials; NOAA; release testing; sawing

Introduction

Nanotechnology is a fast-growing and rapidly advancing technology, impacting global industry and society with numerous new manufactured nanomaterials and products containing these nanomaterials (Schulte *et al*., 2016). Nanotechnology is moving from small research and development (R and D) scale to larger industrial scale (Invernizzi, 2011), but the physical and chemical properties of manufactured nano-objects (MNOs) raise health-related concerns (NIOSH, 2013).

The potential exposure of workers to manufactured nano-objects, their agglomerates, and aggregates (NOAA) has received considerable attention in recent years (Debia *et al*., 2016; Kuijpers *et al*., 2017), as occupational exposure levels are normally higher than consumer exposure levels and their safety is a cornerstone of responsible innovation. According to Schneider *et al*. (2011), occupational activities with MNO cover the whole life cycle of a nanotechnology-based product, which can be divided into four stages, namely (i) synthesis of MNO, (ii) handling and transfer of MNO, (iii) application of products containing MNO, and (iv) fracturing and abrasion of products that include MNO. In contrast to workers involved in the first stages of the product life cycle, the awareness of end users about the presence of MNOs in their products is relatively low (Broekhuizen *et al*., 2011). Increasing awareness requires more knowledge about scenarios with quantitative release of NOAA (Koivisto *et al*., 2017).

Previous studies on the exposure potential of NOAA during the final stage (4) fracturing and abrasion predominantly focused on sanding activities on products containing multi-walled carbon nanotubes (MWCNTs) and silica (Bello, 2009; Koponen *et al*., 2009; Vorbau *et al*., 2009; Göhler *et al*., 2010, Koponen *et al*., 2011; Huang *et al*., 2012; Gomez *et al*., 2014; Fransman *et al*., 2016; Koivisto, *et al*., 2017). Only a limited number of (simulated) workplace studies focused on other occupational activities regularly performed, such as sawing (Bello, 2009; Methner *et al*., 2012; Gomez *et al*., 2014; Bekker *et al*., 2015) and solid core drilling activities (Bello *et al*., 2010; Sachse *et al*., 2013). Concentration levels of nanoparticles (including NOAA) were up to 1.6E6 # cm^{-3} and 2.0E5 # cm^{-3} for sawing and drilling, respectively. In general, interpretation of the results from abrasion and fracturing studies is challenging as measurements have shown that particles emitted by electrical tools themselves were repeatedly reported as a major source of nanosize particles (Koponen *et al*., 2009; Broekhuizen *et al*., 2011; Kuhlbusch *et al*., 2011; Wohlleben *et al*., 2011; Fransman *et al*., 2016; Kuijpers *et al*., 2017). More research is needed for realistic risk assessments in the later stages of the life cycle of MNO for activities other than sanding, not influenced by particles emitted by electrical tools themselves.

The objective of this study was to assess the potential exposure (qualitatively morphology and chemical composition and quantitatively particle number concentration and particle size distribution) of NOAAs and other (formulated) nanosized particles during automatic sawing and drilling. For this purpose, real-time aerosol concentrations were measured both in the vicinity and far from the activity in a controlled environment. In total, 12 simulated workplace experiments were completed to investigate various determinates of exposure, namely type of MNO [car bumpers containing nanosized MWCNT or nanosized organic pigment (OP)]; activity (automated sawing or drilling); instrument settings (speed for sawing, drill size for drilling); and mechanical ventilation (on/off). Furthermore, each of the experiments was repeated three times to assess the variability in concentration levels.

Methods

Studied materials

The test materials included two car bumpers: a red high-density polyethylene (HDPE) polymer matrix containing 10 weight percent (wt. %) OP Red 254 and a black polyurethane (PU) matrix containing 0.09 wt. % MWCNT (Sotiriou *et al*., 2016). The OP Red 254 particles have a diameter of 26 nm and a Brunauer Emmet and Teller surface of 94 $m^2\ g^{-1}$. MWCNTs have on average a diameter of 9.5 nm, a length of 1.5 µm, and a BET surface of 250–300 $m^2\ g^{-1}$. Both types of car bumpers have a comparable tensile stress, which is the capacity of the car bumpers to withstand loads tending to elongate (ISO 527-2). Prior to the experiments, the

car bumpers were cut over the length in several parts to create equally sized objects of ca. 50 × 10 × 1 cm. The nanomaterials and car bumpers were tested as one of the selected life-cycle test materials in the FP7 'Sustainable Nanotechnologies' Project (www.sun-fp7.eu).

Experimental set-up and environmental conditions

The experiments were performed in an experimental room of 19.5 m^3 (length 3.90 m × width 2.10 m × height 2.38 m), which was previously described (Fransman *et al.*, 2016; Bekker *et al.*, 2017). Environmental conditions in the room were controlled during the experiments with temperatures and relative humidity ranging from 18 to 22°C and 35 to 42%, respectively. Two different settings of the mechanical ventilation and the effect on concentration levels were evaluated with the experiments: 0 air change per hour (ACH) and 3.5 ACH as determined using an automatic air volume flow meter (TSI, Airflow Instruments ProHood Capture Hood PH731). The test room was flushed between two experiments using the maximum capacity of the mechanical ventilation (~20 ACH) to allow a maximum background concentration prior to every experiment of <200 # cm^{-3} [using Electrical Low Pressure Impactor (ELPI) (+), model 9721 Dekati]. In addition, during this period between the experiments, the room was cleaned with a wet duster and a professional vacuum cleaner with a high-efficiency particulate air filter.

Previous release experiments reported significant particle emissions from electric motors in the machines used for abrasive activities (Koponen *et al.*, 2009; Broekhuizen *et al.*, 2011; Kuhlbusch *et al.*, 2011; Wohlleben *et al.*, 2011; Fransman *et al.*, 2016), which was explained by carbon brushes sliding over copper commutator contacts (Lioy *et al.*, 1999; Szymczak *et al.*, 2007). As these particles influence the results of the release experiments, this study used a bandsaw table and a drill table both with an induction motor. These induction motors were selected, as no particles are emitted by the motor, which was confirmed in the experimental room prior to the experiments. A bandsaw table was used for the sawing experiments (Metabo, BAS 318, EAN 4007430304940) with two different sawing speeds (410 and 880 m min^{-1}). The drill table used for the drilling experiments (Dedra DED7708, EAN 5902628770806) was operated (2700 r.p.m) using two different titanium drill bits (4 and 8 mm).

The total measurement duration of every experiment was 13 min and consisted of 5 min of background measurements before the activity (phase 1), followed by 3 min of the activity (phase 2) and 5 min after the activity (phase 3). The fieldworker that performed the tests was in the experimental room during the entire experiment, using respirator protective equipment (P3 filter). To standardize the experiments, the numbers and duration of drill holes and the sawed length were equal in every experiment. An overview of the performed experiments and the studied variables is shown in Table 1. We performed four different experiments (all performed in triplicate) using the drill table, varying the type of car bumper (MWCNT or OP) and drill size (4 and 8 mm). Eight different experiments (in triplicate) were completed using the band-saw table, varying the nanomaterial (MWCNT or OP) in the car bumper, sawing speed (410 and 880 m min^{-1}), and mechanical ventilation [0 and 3.5 ACH (only for sawing)].

Instrumentation

All measurement instruments were placed outside the room and attached with anti-static sampling tubes or with the tube type as provided by the instrument (<50 cm) to minimize the effect of the instruments on the experimental results. The inlets of the instruments were placed as close as possible to the source (near field; NF, ~20 cm) or in the opposite corner of the room (~4 m, far field; FF). All instrument types were used for measurements at both the NF and FF measurement locations. For a schematic overview of the experimental set-up and the position of the instruments, see Supplementary Figure 1 (available at *Annals of Work Exposures and Health* online).

Inhalable dust particles were collected on 25-mm nickel-coated nucleopore filters (pore size 0.4 µm) for morphology, chemical composition, and size using an IOM sampler and a volume flow of 2 l min^{-1} provided by Buck Basic-5MH pumps. Filters were loaded only

Table 1. Summary determinates and variables.

Determinants	Variables
Car bumper	Red HDPE matrix with 10 wt. % OP
	Black PU matrix with 0.09 wt. % MWCNT
Abrasive machines	Bandsaw table
	Drill table
Machine settings	Speed for sawing (410 and 880 m min^{-1})
	Drill size for drilling (4 and 8 mm)
Mechanical ventilation	0 ACH
	3.5 ACH (only for sawing)

HDPE = high density polyethylene; OP = organic pigment; PU = polyurethane; MWCNT = multi-walled carbon nanotubes; ACH = air change per hour.

during phase 2 and 3 and triplicate experiments were combined on one filter resulting in a total sampling duration of 24 min (48 l) per filter. Only a selection of the filters collected in the NF were analysed by scanning electron microscope (SEM, model MIRA-LMH, Tescan) and in situ chemical analysis by energy-dispersive X-ray spectrometry (EDX spectrometer with XFlash 4010 detector; Bruker), as similar qualitative results may be expected in the FF.

In order to quantify the concentration levels, particle number concentrations were assessed in the range of 10–300 nm using the DiSCmini (Matter Aerosol, Switzerland). In addition, the particle size distributions were measured using a Scanning Mobility Particle Sizer (SMPS, model 3936 with long DMA model 3081 and water CPC 3786, TSI Inc.), an Aerodynamic Particle Sizer (APS model 3321, TSI Inc.), and an ELPI + (NF) and ELPI (FF) (Model 9721, Dekati). The measured size range and response time for the SMPS, APS, ELPI, and ELPI (+) were 11.3–514 nm (1 min), 0.5–20 µm (1 s), 0.007–10 µm (1 s), and 0.006–10 µm (1 s), respectively. Due to technical issues, no data were collected for four experiments with the ELPI + and for one experiment with the SMPS. Results for particle size distributions were normalized to dN/dlogDp to compare the distributions taken of the same aerosol using different instruments with different size resolutions (mobility or aerodynamic diameter).

Statistical analyses

The methodology to analyse the particle number concentrations collected with the DiSCmini and the particle size distributions sampled with the SMPS, APS, and ELPI (+) was previously described by Bekker *et al.*, 2017. In brief, a two-stage modelling strategy was applied: in stage 1, an autoregressive integrated moving average (ARIMA) model was used for individual experiments; in stage 2 the individual results of stage 1 were combined to evaluate and quantify the effect of the different determinants and variables.

In stage 1, ARIMA models were used to take into account the pattern of autocorrelation in the sequential measurements collected with real-time instruments. In a stepwise approach that was previously described by Klein Entink *et al.* (2011) and Klein Entink *et al.* (2015), the data were forced for stationarity as assumed by an ARIMA model. A second-order moving-average model was applied (100 iterations), which had the best fit with the measurement data. In addition, the data set included for every data point a binary (0, 1) variable, to indicate the data related to the background and the activity. As a result, model estimates were derived for both the average background and the average activity number concentration (DiSCmini) or size distribution (SMPS, APS, and ELPI (+)). Next, activity-effect estimates (β) and standard error (SE) were used in stage 2 of the analysis.

In stage 2, it was assumed that the uncertainty in the stage 1 results is characterized by a lognormal model with the estimated mean (β) and SE. To account for this uncertainty, a Monte Carlo simulation was performed randomly selecting values (n = 1000) from the distribution. The selected values were used in a multiple linear regression model with the evaluated determinants as independent variables. Regression coefficients (β) and SE were pooled per experiment. Finally, β results were exponentiated (by squaring) to obtain geometric mean ratios (GMR). All statistical analyses were performed in R studio version 3.1.2 (R Core Team, 2014).

Results

Characterization of released particles

In total, 24 nickel-coated nucleopore filters (12 different experiments, both NF and FF) were collected of which only 6 filters were analysed by analytical SEM, focusing first on the filters with the highest particle loading. The filters selected to qualify the release were all collected in the NF of the experiments, with three filters for the red car bumper containing OP and with three filters for the black car bumper containing MWCNTs. The three filters for both the red and black car bumper varied in the abrasive activities performed during the experiments (N = 2 × 2 for sawing, N = 2 × 1 for drilling). The filters for the sawing experiments varied in the bandsaw table setting (speed 410 and 880 m min^{-1}), whereas for drilling only the filters for the 8-mm drill bit were analysed. In general, no MWCNTs and OP particles were observed to be liberated from the matrix. Furthermore, for the drilling experiments no activity-related particles from the test materials were observed. But, for the sawing experiments activity-related carbon-rich particles were observed as spherical conglomerates with sizes between ~100 and 20 µm (but mainly between ~2 and ~8 µm), which included either MWCNT or OP. These results can be extrapolated to the filters collected during other experiments, which were not analysed, as the morphology, chemical composition, and size of emitted particles are expected to be comparable. The smooth surface of the observed particles can be explained by heat production of the bandsaw table, which (partly) melted the abrasively treated objects. Figure 1 shows four examples of the observed activity-related particles for the sawing experiments. Fragments of the OP

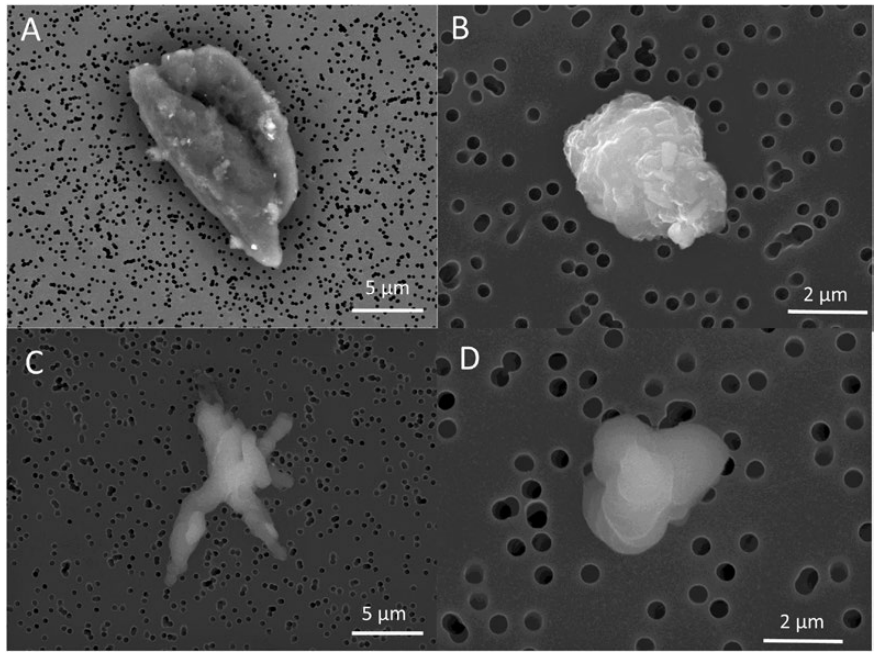

Figure 1. Four examples of activity related released matrix particles for sawing, with a smooth surface morphology, (partly) melted due to the bandsaw table. In 1A and 1B organic pigment (OP) containing high density polyethylene (HDPE) matrix fragments, in 1C and 1D MWCNT containing polyurethane (PU) matrix fragments.

containing HDPE matrix are shown in Fig. 1A and B, whereas MWCNTs containing PU matrix fragments are shown in Fig. 1C and D.

Activity-effect estimates

During the drilling experiments, relatively low particle number concentrations were measured (DiSCmini, <800 # cm^{-3}) as compared to background concentrations (100–200 # cm^{-3}), whereas no (visual) differences were observed in particle size distributions [10 nm–20 µm; SMPS, APS, ELPI (+)]. For the sawing experiments, relatively high particle number concentrations were found (DiSCmini, up to 1.2E6 # cm^{-3}) as compared to comparable background levels (100–200 # cm^{-3}). Visual differences in particle size distributions were observed (based on comparing the individual graphs) in the SMPS, APS, and ELPI (+) data with more detected particles between 10 and ~200 nm compared to background concentrations.

In Table 2, the average particle number concentration and particle size are available per triplicated experiments per instrument in NF and FF using the stage 1 ARIMA models. Individual results of the experiments geometric mean (GM) and geometric standard deviation (GSD) and the results of the statistical analyses of the individual experiments (stage 1) are available in Supplementary Tables 1–4 (available at *Annals of Work Exposures and Health* online). The regression models (second stage) for drilling activities showed no significant relation between number concentrations, particle size distributions, and the studied determinants (type of car bumper, machine settings) and corresponding variables (red HDPE matrix with 10 wt. % OP versus black PU matrix with 0.09 wt. % MWCNT, drill size 4 mm versus 8 mm) in the NF (Table 3) and the FF (Table 3). Significant differences in particle number concentrations and particle size distributions were found for the sawing experiments in the NF (Table 4) and the FF (Table 4). Regarding the number concentrations, a higher sawing speed (880 versus 410 m min^{-1}) resulted in significantly higher concentrations with GMRs of 59 (P = < 0.01) and 22 (P = < 0.01) in NF and FF, respectively. In the FF a significantly higher concentration was found for the car bumpers containing OP compared to the ones containing MWCNTs (GMR = 0.45, P = 0.02), but results were not statistically significant in the NF although the direction of the effect was similar (GMR = 0.92, P = 0.81). This finding is most likely explained by the operator in the experimental room who influenced the airflows more in the NF compared to the FF. General room ventilation at 3.5 ACH reduced the particle number concentration in air when the ventilation was active, but results were only borderline statistically significant (GMR 0.53, P = 0.06). Regarding the particle size distributions, the

Table 2. Average particle number concentrations (# cm^{-3}) and particle size (nm or μm) with GM and GSD results averaged for the triplicated experiments, with NF and FF results.

NF

Exp. No.	DiSCmini		SMPS		APS		ELPI +	
	GM (#cm^{-3})	GSD	GM (nm)	GSD	GM (μm)	GSD	GM (nm)	GSD
1–3	11.81	1.78	60.13	1.02	1.00	1.04	10.92	1.04
4–6	93.19	1.51	57.56	1.04	0.99	1.07	12.07	1.10
7–9	77.86	2.29	55.82	1.01	0.97	1.07	13.79	1.15
10–12	0	1.92	13.72	1.06	0.98	1.08	—	—
13–15	17820.71	2.21	34.83	1.57	1.07	1.06	14.31	1.49
16–18	15926.93	1.98	39.84	1.38	1.10	1.07	11.50	1.20
19–21	24411.93	1.86	29.12	1.49	1.11	1.04	15.85	1.16
22–24	28675.76	1.66	37.92	1.43	1.09	1.05	20.97	1.35
25–27	492746.53	2.64	24.31	1.41	1.09	1.05	6.46*	1.32
28–30	250611.98	2.13	29.02	1.96	0.99	1.04	10.91	2.20
31–33	501365.62	1.99	31.90	1.32	0.96	1.05	10.36	1.04
34–36	311600.73	2.02	28.24	1.90	1.02	1.05	11.19	1.10

FF

Exp. No.	DiSCmini		SMPS		APS		ELPI	
	GM (# cm^{-3})	GSD	GM (nm)	GSD	GM (μm)	GSD	GM (nm)	GSD
1–3	0	1.89	62.79	1.06	1.17	1.07	47.58	1.35
4–6	0	1.74	58.65	1.03	1.07	1.07	47.22	1.20
7–9	0	1.14	55.11	1.02	1.03	1.10	55.61	1.09
10–12	0	1.13	13.82	1.02	1.04	1.09	42.49	1.08
13–15	2498.07	1.79	33.28	1.67	1.22	1.08	53.71	1.20
16–18	3507.45	2.11	37.20	1.36	1.31	1.09	55.86	1.31
19–21	4601.84	2.29	35.03	1.40	1.28	1.06	55.22	1.09
22–24	5758.37	2.08	31.16	1.77	1.22	1.08	68.44	1.24
25–27	147676.90	4.08	25.14	1.49	1.23	1.06	44.61	1.18
28–30	46979.95	2.78	22.22	1.33	1.10	1.07	44.12	1.16
31–33	90240.11	3.67	36.58	1.53	1.12	1.09	46.14	1.19
34–36	86562.76	2.91	28.86	1.95	1.15	1.09	55.18	1.17

GM = geometric mean; GSD = geometric standard deviation; NF = near field; FF = far field.

ELPI + showed smaller particles for higher sawing speed in the NF (GMR = 1.15, $P = 0.01$), whereas in the FF larger particles were found for MWCNT-containing car bumpers (GMR = 0.92, $P < 0.01$) and higher sawing speed (GMR = 1.08, $P < 0.01$), and smaller particles with ventilation (GMR = 0.86, $P < 0.01$).

Discussion

This study provides a comprehensive overview of simulated occupational sawing and drilling in car bumpers containing either OP or MWCNTs, testing the effect of different variables on the concentration levels measured in the NF and FF, which included machine settings and mechanical ventilation. The controlled experimental environment, no disturbing particle emissions from the sawing and drilling machines, a consistently used method (in triplicate) of data collection, and the detailed statistical analyses allowed to study the contribution of potential determinants of the release of MNO both in the NF and FF. SEM/EDX analyses of filters collected during sawing revealed (partly melted) carbon-rich particles as spherical conglomerates (~100 nm–20 μm but mainly between ~2 and ~8 μm), whereas for drilling no activity-related particles were observed. A higher sawing speed significantly contributed to more particles released, both in NF and FF. Ventilation reduced the particle number concentration and shifted

Table 3. Activity-effect estimates for drilling experiments with NF and FF results. In bold, markers determinants ($P < 0.05$) associations with air concentrations.

NF

Instruments	Determinant	GMR	SE	*P*-value
Number concentrationDiSCmini:	Material: MWCNTs versus OP	1.02	1.41	0.94
10–300 nm	Drilling size: 4 versus 8 mm	0.75	1.41	0.40
Particle sizeSMPS, 11.3–514 nm	Material: MWCNTs versus OP	1.14	3.61	0.92
	Drilling size: 4 versus 8 mm	1.03	3.53	0.98
Particle sizeAPS, 500 nm–20 µm	Material: MWCNTs versus OP	1.06	1.09	0.49
	Drilling size: 4 versus 8 mm	0.98	1.09	0.85
Particle sizeELPI +, 6 nm–10 µm	Material: MWCNTs versus OP	1.03	1.03	0.25
	Drilling size: 4 versus 8 mm	1.02	1.03	0.43

FF

Instruments	Determinant	GMR	SE	*P*-value
Number concentrationDiSCmini:	Material: MWCNTs versus OP	0.86	1.15	0.28
10–300 nm	Drilling size: 4 versus 8 mm	1.08	1.15	0.57
Particle sizeSMPS, 11.3–514 nm	Material: MWCNTs versus OP	0.86	4.15	0.92
	Drilling size: 4 versus 8 mm	1.01	4.18	0.99
Particle sizeAPS, 500 nm–20 µm	Material: MWCNTs versus OP	0.95	1.10	0.59
	Drilling size: 4 versus 8 mm	1.04	1.10	0.71
Particle sizeELPI, 7 nm–10 µm	Material: MWCNTs versus OP	0.93	1.04	0.09
	Drilling size: 4 versus 8 mm	0.99	1.04	0.87

the particle size distribution to larger particles when the ventilation was active, but results were only significant for the particle size distribution in the FF. The car bumpers containing MWCNTs showed fewer released particles for the sawing experiments, but only significant in the FF.

In two other comparable drilling experiments, different composites were investigated, which included nanosized silica, nanoclay, microsized polyamide, and polypropylene composites (Sachse *et al.*, 2012; Sachse *et al.*, 2013). In both studies, a handheld Makita angle drill was situated outside of the experimental testing room. Although the authors found large differences in dust generation between the different tested composites, the results were not conclusive on the effect of nanoparticles on the tensile stress of the composites and the type(s) of released particles explaining the differences in generated particles. Bello *et al.* (2010) studied exposures to nanoparticles and nanofibres during drilling of two types of hybrid composites containing aluminium or carbon fibres and carbon nanotube (CNT). This study revealed airborne clusters of CNTs and ultra-fine (<5 nm) aerosols due to thermal degradation of the composite material. Both higher input energy and the type of the composite were identified as an important exposure modifying factor, with CNT-composites generally having a tendency to release less particles. The authors recommended additional work for a better understanding of the contributing particles on the total particles released. In contrast, in this study we showed no significant release of airborne particles during drilling activities. Although a subtle effect on particle release due to drilling activities cannot be excluded, no concentrations up to 2E5 #cm^{-3} were found, as observed by the previous studies (Bello *et al.*, 2010; Sachse *et al.*, 2012; Sachse *et al.*, 2013). These contradicting results can be explained by differences in drilling methods with the settings of the machines (e.g. drill size and drill speed) and the characteristics of composites that contained MNO (e.g. the thickness of the sample drilled, tensile stress).

Sawing activities at the workplace were measured in two different studies (Methner *et al.*, 2012; Bekker *et al.*, 2015) with exposure to NOAA of 2000 and 3000 # cm^{-3}, respectively. In two experimental studies, sawing activities were simulated (Bello 2009; Gomez *et al.*, 2014). Bello (2009) evaluated sawing using hybrid advanced composites that included CNTs, but did not observe CNTs or bundles of fibres. Ultra-fine particles

Table 4. Activity-effect estimates for sawing experiments with NF and FF results. In bold, markers determinants ($P < 0.05$) associations with air concentrations.

NF

Instrument	Determinant	GMR	SE	*P*-value
Number concentration	Material: MWCNTs versus OP	0.92	1.41	0.81
DiSCmini: 10–300 nm	**Sawing speed: 410 versus 880 m min^{-1}**	**58.73**	**1.41**	**<0.01**
	Ventilation: 0 ACH versus 3.5 ACH	0.53	1.41	0.06
Particle size	Material: MWCNTs versus OP	0.86	2.18	0.85
SMPS, 11.3–514 nm	Sawing speed: 410 versus 880 m min^{-1}	0.77	2.12	0.73
	Ventilation: 0 ACH versus 3.5 ACH	0.96	2.13	0.96
Particle size	Material: MWCNTs versus OP	0.98	1.04	0.64
APS, 500 nm–20 µm	Sawing speed: 410 versus 880 m min^{-1}	0.95	1.04	0.23
	Ventilation: 0 ACH versus 3.5 ACH	1.01	1.04	0.72
Particle size	Material: MWCNTs versus OP	0.91	1.05	0.06
ELPI +, 6 nm–10 µm	**Sawing speed: 410 versus 880 m min^{-1}**	**1.15**	**1.05**	**0.01**
	Ventilation: 0 ACH versus 3.5 ACH	0.96	1.05	0.45

FF

Instrument	Determinant	GMR	SE	*P*-value
Number concentration	**Material: MWCNTs versus OP**	**0.45**	**1.42**	**0.02**
DiSCmini: 10–300 nm	**Sawing speed: 410 versus 880 m min^{-1}**	**22.07**	**1.43**	**<0.01**
	Ventilation: 0 ACH versus 3.5 ACH	0.74	1.42	0.39
Particle size	Material: MWCNTs versus OP	1.06	2.16	0.94
SMPS, 11.3–514 nm	Sawing speed: 410 versus 880 m min^{-1}	0.85	2.16	0.84
	Ventilation: 0 ACH versus 3.5 ACH	1.15	2.18	0.86
Particle size	Material: MWCNTs versus OP	0.96	1.04	0.28
APS, 500 nm–20 µm	Sawing speed: 410 versus 880 m min^{-1}	0.94	1.04	0.11
	Ventilation: 0 ACH versus 3.5 ACH	1.02	1.04	0.57
Particle size	**Material: MWCNTs versus OP**	**0.92**	**1.02**	**<0.01**
ELPI, 7 nm–10 µm	**Sawing speed: 410 versus 880 m min^{-1}**	**1.08**	**1.02**	**<0.01**
	Ventilation: 0 ACH versus 3.5 ACH	**0.86**	**1.02**	**<0.01**

were detected, which were correlated to the different matrix thicknesses tested. Gomez *et al.* (2014) studied the particle release effect of sawing with epoxy and paint nanocomposites, which included CNTs. The sawing tests were performed with a Skil Masters (4585) jig saw. The different number concentrations with ELPI varied between 1.2E6 and 1.6E6 # cm^{-3}, which the authors explained by different hardness of the testing materials and subsequent differences in the motor load of the saw. These experimental studies support our data, but the relatively low concentrations found in the actual workplace deviate from our findings. Where Methner *et al.* (2012) and Bekker *et al.* (2015) performed personal measurements, the experimental studies including ours used stationary measurements in the NF and FF. These deviations may be explained by differences in the sawed material, the sawing machine, and the circumstances at the workplace that is normally not comparable to a testing room.

In this research, we showed the effect of potential exposure determinants. Energy level (sawing speed) had a significant effect on both the particle number concentration and the particle size distribution. Ding and Riediker (2015) evaluated the stability of particles with increasing energy levels, using different types of nanomaterials. An increasing energy applied to the materials was related to higher number concentrations and smaller airborne particles (11–1083 nm), which was in agreement with our findings. Although not always significantly different, mechanical ventilation showed lower concentrations when comparing 3.5–0 ACH. The effect of mechanical ventilation as an exposure control for chemical substances was studied and summarized in ECEL and varied between a 35 and 83% reduction

(Fransman *et al*., 2008). The authors are not aware of specific information on the mitigation of exposure to nanomaterials using mechanical ventilation. In this study, the (non-significant) effect for sawing was 47% in the NF (GMR = 0.53, P = 0.06) and 26% in the FF (GMR = 0.74, P = 0.39). However, such values are strongly dependent on room size and the effective speed of mixing of air in the study area.

Studying the release of NOAA due to abrasive activities on MNO-containing materials in relation to real workplace situations will continue to be challenging as a large variation exists in treated materials, processes, and circumstances at the workplace, subsequently influencing potential exposure. Taking this into consideration, the strengths of this study are the use of tools with no particle emissions potentially disturbing the experiments, the relative large number of experiments, and the thorough statistical analyses. In addition, the reproducibility and repeatability of the results were good comparing the individual results of the three experiments performed in triplicate (see Supplementary Tables 1–4, available at *Annals of Work Exposures and Health* online). For release rate measurements, it is preferred to have direct sampling of the emission from the source or homogeneously mixed air from the source. The actual release rates in this study can only be backwards modelled and currently represent concentrations levels (Koivisto *et al*., 2017). Although experiments studying the release rates are relevant for modelling the human and environmental risks, the derived effects of the different determinants in this study are directly applicable to the actual workplace. Also, the effect of ventilation on nanoparticle concentrations in air cannot be tested with release measurements, but needs more quantitative data as its effectiveness for NOAA is currently only limited tested (Goede *et al*., 2018). The three instruments we used for the particle size distribution [SMPS, APS, and ELPI(+)] varied in the measured size range, response time, and working mechanism, which resulted in different outcomes. Ideally, these instruments show similar trends and it should be possible to compare results and be conclusive about the outcomes. However, no significant results were found for the APS as the measurement range is 0.5–20 µm, whereas mostly small particles were detected. In addition, the SMPS had a response time of 1 min, meaning only a limited number of data were collected per experiment, which resulted in relatively large SEs. Due to the advantages and disadvantages of each instrument, a combination of direct reading instruments (for particle number concentrations and particle size distributions) is still recommended in future research. In addition, offline analyses are needed as none of the currently available direct reading instruments are specific and distinguishes between particle types (e.g. process- and non-process-related nanoparticles).

Conclusion

The experiments in this study give a first indication of the effect of the evaluated determinants on NOAA release during sawing and drilling in polymer car bumpers and consequently on the potential worker exposure. An increase in the energy level of the abrasive activity results in melted carbon-rich particles during sawing, but the added nanomaterials were not liberated from matrix. Mechanical ventilation was (somewhat) effective in the reduction of exposure, whereas no differences in release were found for car bumpers with different MNO of the same tensile stress. Although this study was conducted in an experimental setting, the outcomes are translatable to similar processes in a non-experimental setting such as the workplace or a consumer scenario. As the toxicological properties of the released particles are still unknown, future efforts are needed to properly protect workers, which should aim for realistic risk assessments not only focused on the pristine engineered particles.

Supplementary Data

Supplementary data are available at *Annals of Work Exposures and Health* online.

Acknowledgements

We would like to acknowledge the EU Commission FP7 Program for funding this project (Grant agreement No: 604305). We thank Ilse Tuinman and Marcel Moerman for their contributions during the experiments and we thank Annemarie Prins for assisting with the statistical analysis.

Conflict of Interest

The authors declare no conflict of interest. None of the authors has a financial relationship with a commercial entity that has an interest in the subject of this article.

References

Bekker C, Fransman W, Boessen R *et al.* (2017) Assessment of determinants of emission potentially affecting the concentration of airborne nano-objects and their agglomerates and aggregates. *Ann Work Expo Health*; **61**: 98–109.

Bekker C, Kuijpers E, Brouwer D *et al.* (2015) Occupational exposure to nano-objects and their agglomerates and aggregates across various life cycle stages; A broad-scale exposure study. *Ann Occup Hyg*; **59**: 681–704. doi:10.1093/annhyg/mev023.

Bello D. (2009) Exposure to nanoscale particles and fibers during machining of hybrid advanced composites containing carbon nanotubes. *J Nanopart Res*; **11**: 231–49.

Bello D, Wardle BL, Zhang J *et al.* (2010) Characterization of exposures to nanoscale particles and fibers during solid core drilling of hybrid carbon nanotube advanced composites. *Int J Occup Environ Health*; **16**: 434–50.

Broekhuizen JC, Broekhuizen FA, Cornelissen RTM *et al.* (2011) Use of nanomaterials in the European construction industry and some occupational health aspects thereof. *J Nanopart Res*; **11**: 447–62.

Debia M, Bakhiyi B, Ostiguy C *et al.* (2016) A systematic review of reported exposure to engineered nanomaterials. *Ann Occup Hyg*; **60**: 916–35.

Ding Y,Riediker M. (2015) A system to assess the stability of airborne nanoparticle agglomerates under aerodynamic shear. *J Aerosol Sci*; **88**: 98–108.

Fransman W, Bekker C, Tromp P *et al.* (2016) Potential release of manufactured nano objects during sanding of nano-coated wood surfaces. *Ann Occup Hyg*; **60**: 875–84.

Fransman W, Schinkel J, Meijster T *et al.* (2008) Development and evaluation of an exposure control efficacy library (ECEL). *Ann Occup Hyg*; **52**: 567–75.

Goede H, Christopher-de Vries Y, Kuijpers E *et al.* (2018) A review of workplace risk management measures for nanomaterials to mitigate inhalation and dermal exposure. *Ann Work Expo Health*; **62**: 907–22..

Göhler D, Stintz M, Hillemann L *et al.* (2010) Characterization of nanoparticle release from surface coatings by the simulation of a sanding process. *Ann Occup Hyg*; **54**: 615–24.

Gomez V, Levin M, Saber AT *et al.* (2014) Comparison of dust release from epoxy and paint nanocomposites and conventional products during sanding and sawing. *Ann Occup Hyg*; **58**: 983–94.

Huang G, Park JH, Cena LG *et al.* (2012) Evaluation of airborne particle emissions from commercial products containing carbon nanotubes. *J Nanopart Res*; **14**. pii: 1231. Epub 2012 Oct 20.

Invernizzi N. (2011) Nanotechnology between the lab and the shop floor: what are the effects on labor? *J Nanopart Res*; **13**: 2249–68.

Klein Entink RH, Bekker C, Fransman WF *et al.* (2015) Analysis of time series of particle size distributions in nano exposure assessment. *J Aerosol Sci*; **81**: 62–9.

Klein Entink RH, Fransman W, Brouwer DH. (2011) How to statistically analyze nano exposure measurement results: using an ARIMA time series approach. *J Nanopart Res*; **13**: 6991–7004.

Koivisto AJ, Jensen ACØ, Kling KI *et al.* (2017) Quantitative material releases from products and articles containing manufactured nanomaterials: towards a release library. *NanoImpact*; **5**: 119–32.

Koponen IK, Jensen KA, Schneider T. (2009) Sanding dust from nanoparticle-containing paints: physical characterisation. *J Phys Conf Ser*; **151**.

Koponen IK, Jensen KA, Schneider T. (2011) Comparison of dust released from sanding conventional and nanoparticle-doped wall and wood coatings. *J Expo Sci Environ Epidemiol*; **21**: 408–18.

Kuhlbusch TA, Asbach C, Fissan H *et al.* (2011) Nanoparticle exposure at nanotechnology workplaces: a review. *Part Fibre Toxicol*; **8**: 22.

Kuijpers E, Bekker C, Brouwer D *et al.* (2017) Understanding workers' exposure: systematic review and data-analysis of emission potential for NOAA. *J Occup Environ Hyg*; **14**: 349–59.

Lioy PJ, Wainman T, Zhang J *et al.* (1999) Typical household vacuum cleaners: the collection efficiency and emissions characteristics for fine particles. *J Air Waste Manag Assoc*; **49**: 200–6.

Methner M, Crawford C, Geraci C. (2012) Evaluation of the potential airborne release of carbon nanofibers during the preparation, grinding, and cutting of epoxy-based nanocomposite material. *J Occup Environ Hyg*; **9**: 308–18.

NIOSH. (2013) Occupational exposure to carbon nanotubes and nanofibers. *Curr Intelligence Bull*; **65**: 145.

R Development Core Team. (2014) R: A Language and Environment for Statistical Computing. R Foundation for Statistical Computing, Vienna, Austria.

Sachse S, Gendre L, Silva F *et al.* (2013) On nanoparticles release from polymer nanocomposites for applications in lightweight automotive components. *J Phys Conf Ser*; **429**.

Sachse S, Silva F, Zhu H *et al.* (2012) The effect of nanoclay on dust generation during drilling of PA6 nanocomposites. *J Nanomater*; 2012: 8.

Schneider T, Brouwer DH, Koponen IK *et al.* (2011) Conceptual model for assessment of inhalation exposure to manufactured nanoparticles. *J Expo Sci Environ Epidemiol*; **21**: 450–63.

Schulte PA, Roth G, Hodson LL *et al.* (2016) Taking stock of the occupational safety and health challenges of nanotechnology: 2000–2015. *J Nanopart Res*; **18**: 159.

Sotiriou GA, Singh D, Zhang F *et al.* (2016) Thermal decomposition of nano-enabled thermoplastics: possible environmental health and safety implications. *J Hazard Mater*; **305**: 87–95.

Szymczak W, Menzel N, Keck L. (2007) Emission of ultrafine copper particles by universal motors controlled by phase angle modulation. *J Aerosol Sci*; **38**: 520–31.

Vorbau M, Hillemann L, Stintz M. (2009) Method for the characterization of the abrasion induced nanoparticle release into air from surface coatings. *J Aerosol Sci*; **40**: 209–17.

Wohlleben W, Brill S, Meier MW *et al.* (2011) On the lifecycle of nanocomposites: comparing released fragments and their in-vivo hazards from three release mechanisms and four nanocomposites. *Small*; **7**: 2384–95.

Online Supplementary Material

Relative differences in concentration levels during sawing and drilling of car bumpers containing MWCNT and organic pigment.

Eelco Kuijpers[1,2], Anjoeka Pronk[1], Antti Joonas Koivisto[3], Keld Alstrup Jensen[3], Roel Vermeulen[2], Wouter Fransman[1]

1. TNO, Zeist, The Netherlands.
2. Division of Environmental Epidemiology, Institute for Risk Assessment Sciences, Utrecht University, The Netherlands.
3. National Research Centre for the Working Environment, Lerso Parkallé 105, DK-2100 Copenhagen, Denmark

Corresponding author:

Eelco Kuijpers

TNO, PO box 360, Zeist, The Netherlands

eelco.kuijpers@tno.nl

Figure S1: Schematic layout of experimental setup including position of monitors SMPS, APS, ELPI(+), DISCmini (DM) and sampler (IOM).

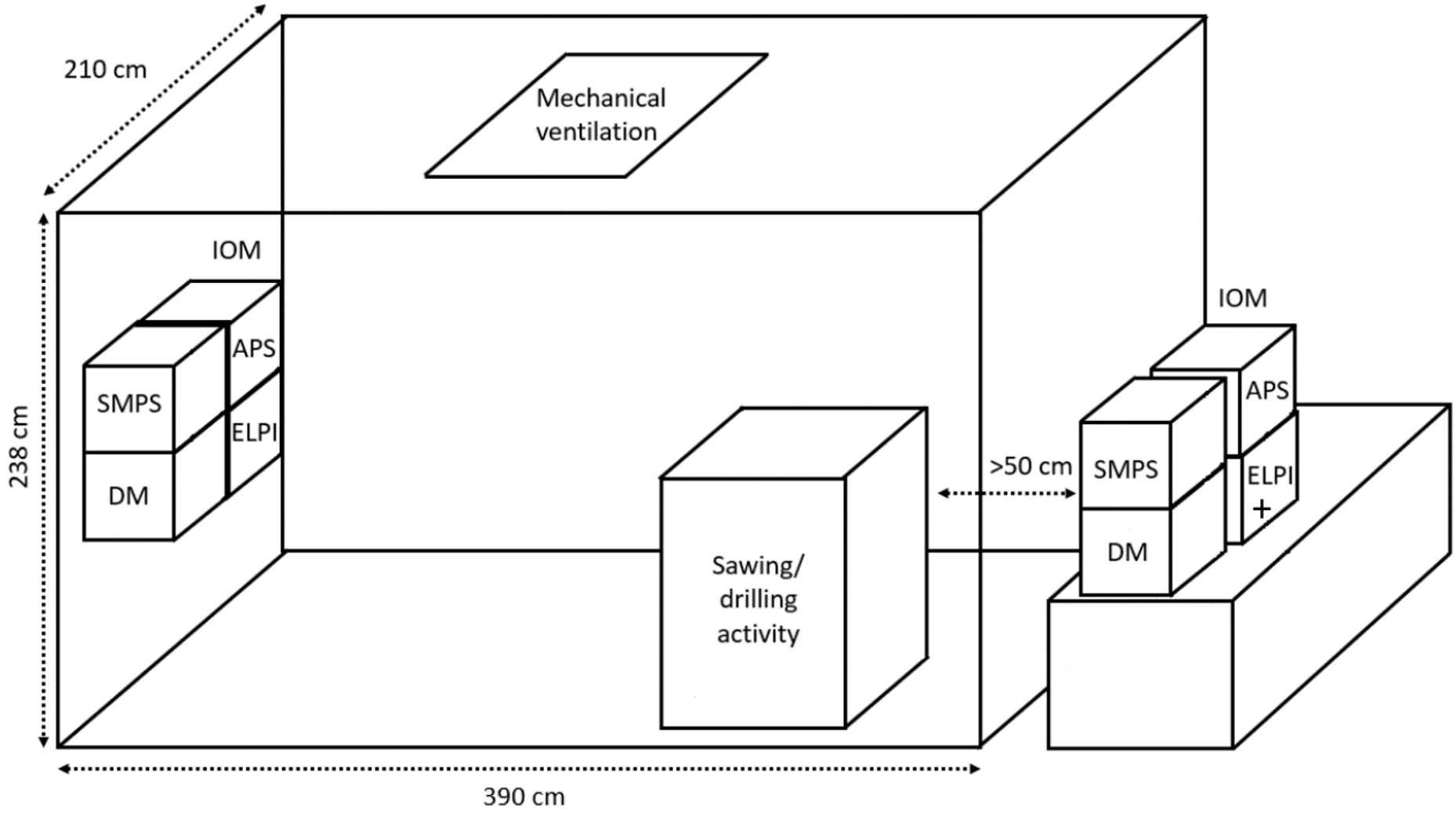

Table S1: Original results of the particle number concentration per experiment (GM and GSD) and results of the first stage analyses for DiSCmini estimated β and SE (log-transformed) of the activity-effect level (background corrected) and determinants.

	Activity-effect level NF				Activity-effect level FF				Exposure determinants			
Exp. No.	**GM (#/cm^3)**	**GSD**	**Mean (β)**	**Standard error (SE)**	**GM (#/cm^3)**	**GSD**	**Mean (β)**	**Standard error (SE)**	**Activity**	**Car bumper**	**Settings machine**	**Mechanical ventilation**
1	2.67	2.08	0.01	0.13	0	2.11	-0.39	0.05	Drilling	MWCNT	Drill size 4 mm	0 ACH
2	29.86	1.56	0.08	0.17	0	1.53	-0.33	0.16	Drilling	MWCNT	Drill size 4 mm	0 ACH
3	20.66	1.75	0.01	0.18	0	2.09	-0.32	0.10	Drilling	MWCNT	Drill size 4 mm	0 ACH
4	127.45	1.41	0.48	0.12	0	1.35	0.08	0.18	Drilling	MWCNT	Drill size 8mm	0 ACH
5	96.92	1.38	0.37	0.15	0	1.72	-0.12	0.15	Drilling	MWCNT	Drill size 8mm	0 ACH
6	65.52	1.78	0.33	0.04	0	2.27	-0.05	0.24	Drilling	MWCNT	Drill size 8mm	0 ACH
7	61.4	2.94	0.56	0.36	0	1.07	-0.02	0.04	Drilling	OP	Drill size 4 mm	0 ACH
8	87.71	1.9	0.78	0.22	0.17	1.14	-0.01	0.05	Drilling	OP	Drill size 4 mm	0 ACH
9	87.64	2.15	0.79	0.29	3.48	1.21	0.14	0.07	Drilling	OP	Drill size 4 mm	0 ACH
10	1.01	2.09	0.03	0.30	0.34	1.13	0.02	0.03	Drilling	OP	Drill size 8mm	0 ACH
11	66.12	1.98	0.34	0.23	0	1.08	-0.12	0.04	Drilling	OP	Drill size 8mm	0 ACH
12	0	1.71	-10.67	0.04	0	1.19	-0.27	0.01	Drilling	OP	Drill size 8mm	0 ACH
13	16978.69	2.48	32.11	0.26	2099.78	2.34	39.64	0.46	Sawing	MWCNT	Sawing speed 410m/min	3.5 ACH
14	20138.56	2.55	35.10	0.25	2487.85	1.56	41.39	0.39	Sawing	MWCNT	Sawing speed 410m/min	3.5 ACH

15	16551.69	1.7	35.41	0.05	2984.11	1.57	46.54	0.26	Sawing	MWCNT	Sawing speed 410m/min	3.5 ACH
16	11946.99	2.6	3.65	0.31	3169.64	2.12	31.29	0.38	Sawing	MWCNT	Sawing speed 880m/min	0 ACH
17	19107.07	1.4	42.49	0.14	3643.5	2.38	32.00	0.42	Sawing	MWCNT	Sawing speed 880m/min	0 ACH
18	17698.80	2.12	42.36	0.22	3736.35	1.85	33.57	0.33	Sawing	MWCNT	Sawing speed 880m/min	0 ACH
19	18223.09	2.72	3.67	0.40	5646.08	2.47	48.20	0.38	Sawing	MWCNT	Sawing speed 410m/min	0 ACH
20	28448.28	1.75	45.40	0.18	4394.86	2.59	49.93	0.28	Sawing	MWCNT	Sawing speed 410m/min	0 ACH
21	28062.63	1.35	45.31	0.12	3927.38	1.88	45.86	0.25	Sawing	MWCNT	Sawing speed 410m/min	0 ACH
22	30936.69	1.34	44.29	0.13	4076.39	2.1	42.49	0.54	Sawing	MWCNT	Sawing speed 880m/min	3.5 ACH
23	27353.53	2.38	41.73	0.29	5551.38	2.6	48.69	0.20	Sawing	MWCNT	Sawing speed 880m/min	3.5 ACH
24	27864.91	1.43	43.13	0.15	8437.64	1.65	55.11	0.18	Sawing	MWCNT	Sawing speed 880m/min	3.5 ACH
25	575611.7	1.78	79.40	0.49	109121.6	8.77	80.29	0.75	Sawing	OP	Sawing speed 410m/min	3.5 ACH
26	652493.9	2.02	80.85	0.50	203920.1	2.52	86.08	0.40	Sawing	OP	Sawing speed 410m/min	3.5 ACH
27	318540.5	5.11	69.00	0.72	144732.8	3.07	79.12	0.58	Sawing	OP	Sawing speed 410m/min	3.5 ACH
28	225283.5	2.88	68.58	0.41	35464.74	2.58	62.03	0.41	Sawing	OP	Sawing speed 880m/min	0 ACH

29	249832.9	2.06	71.42	0.16	54626.25	2.77	67.05	0.44	Sawing	OP	Sawing speed 880m/min	0 ACH
30	279657.5	1.64	72.88	0.20	53522.89	3	68.53	0.44	Sawing	OP	Sawing speed 880m/min	0 ACH
31	489647.7	1.57	81.45	0.25	91953.57	3.44	73.36	0.48	Sawing	OP	Sawing speed 410m/min	0 ACH
32	422143	3.74	78.49	0.48	75687.66	4.44	67.55	0.63	Sawing	OP	Sawing speed 410m/min	0 ACH
33	609705.8	1.35	83.68	0.24	105585.7	3.23	72.38	0.58	Sawing	OP	Sawing speed 410m/min	0 ACH
34	307012.6	1.9	94.84	0.23	97956.56	2.21	77.06	0.20	Sawing	OP	Sawing speed 880m/min	3.5 ACH
35	254985.8	1.88	92.25	0.25	63998.92	3.2	75.99	0.46	Sawing	OP	Sawing speed 880m/min	3.5 ACH
36	386476.6	2.31	96.13	0.29	103463.5	3.49	77.17	0.62	Sawing	OP	Sawing speed 880m/min	3.5 ACH

GM: Geometric mean, GSD: Geometric standard deviation, NF: near field, FF: far field, OP: organic pigment, MWCNT: multi-walled carbon nanotubes, ACH: air change per hour

Table S2: Original results per experiment (GM and GSD) of the particle size and results of the first stage analyses for SMPS estimated β and SE (log-transformed) of the activity-effect level (background corrected) and determinants.

	Activity-effect level NF				**Activity-effect level FF**				**Exposure determinants**			
Exp. No.	**GM (nm)**	**GSD**	**Mean (β)**	**Standard error (SE)**	**GM (nm)**	**GSD**	**Mean (β)**	**Standard error (SE)**	**Activity**	**Car bumper**	**Settings machine**	**Mechanical ventilation**
1	58.77	1.03	-0.13	1.79	63.75	1.08	0.19	1.17	Drilling	MWCNT	Drill size 4 mm	0 ACH
2	60.04	1.02	0.06	0.94	64.98	1.09	-0.09	1.47	Drilling	MWCNT	Drill size 4 mm	0 ACH
3	61.61	1	-0.43	1.59	59.77	1	-1.19	1.91	Drilling	MWCNT	Drill size 4 mm	0 ACH

4	56.22	1.08	-0.26	1.08	60.15	1.06	0.05	1.54	Drilling	MWCNT	Drill size 8mm	0 ACH
5	59.71	1.05	0	1.56	58.40	1.04	-0.07	1.45	Drilling	MWCNT	Drill size 8mm	0 ACH
6	56.81	1	-0.66	2.21	57.42	1	-0.62	2.2	Drilling	MWCNT	Drill size 8mm	0 ACH
7	55.48	1.01	0.11	1.31	56.10	1.02	-0.15	1.5	Drilling	OP	Drill size 4 mm	0 ACH
8	53.29	1.01	0.09	1.17	56.42	1.04	0.17	1.8	Drilling	OP	Drill size 4 mm	0 ACH
9	58.82	1	-0.73	1.61	52.88	1	-0.45	1.92	Drilling	OP	Drill size 4 mm	0 ACH
10	51.17	1.04	0	1.47	52.09	1.05	-0.14	1.11	Drilling	OP	Drill size 8mm	0 ACH
11	50.47	1.09	0.19	1.18	50.66	1	-0.3	1.75	Drilling	OP	Drill size 8mm	0 ACH
12	-	-	-	-	-	-	-	-	Drilling	OP	Drill size 8mm	0 ACH
13	38.33	1.72	-0.71	1.39	35.22	1.89	-0.58	1.36	Sawing	MWCNT	Sawing speed 410m/min	3.5 ACH
14	31.57	1.53	-0.46	1.28	31.65	1.58	-0.61	0.57	Sawing	MWCNT	Sawing speed 410m/min	3.5 ACH
15	34.91	1.47	-0.51	1.18	33.06	1.56	-0.44	0.91	Sawing	MWCNT	Sawing speed 410m/min	3.5 ACH
16	37.92	1.61	-0.37	1.1	31.95	1.58	-0.62	0.64	Sawing	MWCNT	Sawing speed 880m/min	0 ACH
17	34.68	1.64	-0.61	1.34	33.22	1.59	-0.51	1.23	Sawing	MWCNT	Sawing speed 880m/min	0 ACH
18	48.10	1	-0.9	2.08	48.50	1	-0.75	2	Sawing	MWCNT	Sawing speed 880m/min	0 ACH
19	32.72	1.76	-0.62	1.15	32.36	1.78	-0.63	1.34	Sawing	MWCNT	Sawing speed 410m/min	0 ACH
20	30.88	1.65	-0.73	0.89	30.38	1.55	-0.5	1.21	Sawing	MWCNT	Sawing speed 410m/min	0 ACH
21	24.44	1.14	-0.24	1.39	43.72	1	-0.82	1.82	Sawing	MWCNT	Sawing speed 410m/min	0 ACH
22	34.75	1.77	-0.48	1.45	31.72	1.76	-0.63	1.69	Sawing	MWCNT	Sawing speed 880m/min	3.5 ACH
23	30.22	1.64	-0.72	0.89	30.65	1.77	-0.61	1.46	Sawing	MWCNT	Sawing speed 880m/min	3.5 ACH

24	51.93	1	-0.8	1.55	31.13	1.77	-0.88	1.25	Sawing	MWCNT	Sawing speed 880m/min	3.5 ACH
25	28.45	1.91	-0.84	1.15	29.31	2.04	-0.86	1.38	Sawing	OP	Sawing speed 410m/min	3.5 ACH
26	22.69	1.38	-0.55	1.27	25.33	1.61	-0.84	0.94	Sawing	OP	Sawing speed 410m/min	3.5 ACH
27	22.25	1.06	-0.48	1.46	21.41	1	-0.96	1.72	Sawing	OP	Sawing speed 410m/min	3.5 ACH
28	34.03	2.39	-1.13	1.09	33.58	2.32	-0.75	1.68	Sawing	OP	Sawing speed 880m/min	0 ACH
29	29.84	2.10	-1.26	1.24	18.20	1.01	-0.35	1.01	Sawing	OP	Sawing speed 880m/min	0 ACH
30	24.06	1.50	-1	1.01	17.94	1	-0.67	1.67	Sawing	OP	Sawing speed 880m/min	0 ACH
31	58	1.16	-0.89	1.59	62.56	1.06	-0.53	1.46	Sawing	OP	Sawing speed 410m/min	0 ACH
32	25.97	1.53	-0.95	1.2	28.93	1.93	-0.67	1.02	Sawing	OP	Sawing speed 410m/min	0 ACH
33	21.55	1.29	-0.56	1.29	27.05	1.75	-1.05	1.05	Sawing	OP	Sawing speed 410m/min	0 ACH
34	32.58	2.31	-0.87	1.33	34.84	2.56	-1.18	0.9	Sawing	OP	Sawing speed 880m/min	3.5 ACH
35	27.84	1.87	-0.85	1.1	27.18	1.81	-0.67	1.13	Sawing	OP	Sawing speed 880m/min	3.5 ACH
36	24.83	1.60	-0.85	1.35	25.39	1.60	-0.93	1.15	Sawing	OP	Sawing speed 880m/min	3.5 ACH

GM: Geometric mean, GSD: Geometric standard deviation, NF: near field, FF: far field, OP: organic pigment, MWCNT: multi-walled carbon nanotubes, ACH: air change per hour

Table S3: Original results per experiment (GM and GSD) of the particle size and results of the first stage analyses for APS estimated β and SE (log-transformed) of the activity-effect level (background corrected) and determinants.

	Activity-effect level NF				**Activity-effect level FF**				**Exposure determinants**			
Exp. No.	**GM (µm)**	**GSD**	**Mean (β)**	**Standard error (SE)**	**GM (µm)**	**GSD**	**Mean (β)**	**Standard error (SE)**	**Activity**	**Car bumper**	**Settings machine**	**Mechanical ventilation**
1	1.04	1.06	-0.03	0.11	1.28	1.07	-0.07	0.09	Drilling	MWCNT	Drill size 4 mm	0 ACH

2	0.96	1.04	-0.08	0.08	1.14	1.08	-0.17	0.09	Drilling	MWCNT	Drill size 4 mm	0 ACH
3	0.99	1.02	-0.05	0.09	1.10	1.06	-0.19	0.11	Drilling	MWCNT	Drill size 4 mm	0 ACH
4	1.02	1.07	-0.02	0.11	1.19	1.08	0.02	0.1	Drilling	MWCNT	Drill size 8mm	0 ACH
5	0.98	1.08	-0.03	0.12	1.02	1.05	-0.12	0.09	Drilling	MWCNT	Drill size 8mm	0 ACH
6	0.96	1.05	-0.04	0.09	1.00	1.09	-0.15	0.1	Drilling	MWCNT	Drill size 8mm	0 ACH
7	1.04	1.10	0.11	0.12	1.15	1.10	0.04	0.11	Drilling	OP	Drill size 4 mm	0 ACH
8	0.97	1.05	0.04	0.1	1.00	1.13	-0.12	0.1	Drilling	OP	Drill size 4 mm	0 ACH
9	0.90	1.07	-0.02	0.09	0.94	1.08	-0.13	0.14	Drilling	OP	Drill size 4 mm	0 ACH
10	1.04	1.07	0.02	0.11	1.14	1.09	-0.04	0.11	Drilling	OP	Drill size 8mm	0 ACH
11	0.86	1.08	-0.1	0.1	0.86	1.08	-0.11	0.14	Drilling	OP	Drill size 8mm	0 ACH
12	1.06	1.10	0.04	0.08	1.15	1.10	0	0.09	Drilling	OP	Drill size 8mm	0 ACH
13	1.06	1.03	-0.02	0.06	1.16	1.08	-0.12	0.06	Sawing	MWCNT	Sawing speed 410m/min	3.5 ACH
14	1.10	1.10	0.01	0.04	1.29	1.11	0.01	0.05	Sawing	MWCNT	Sawing speed 410m/min	3.5 ACH
15	1.04	1.05	-0.04	0.05	1.20	1.06	-0.07	0.04	Sawing	MWCNT	Sawing speed 410m/min	3.5 ACH
16	1.12	1.06	-0.13	0.06	1.35	1.09	-0.05	0.06	Sawing	MWCNT	Sawing speed 880m/min	0 ACH
17	1.08	1.05	-0.14	0.06	1.26	1.07	-0.11	0.06	Sawing	MWCNT	Sawing speed 880m/min	0 ACH
18	1.11	1.10	-0.12	0.05	1.32	1.11	-0.05	0.06	Sawing	MWCNT	Sawing speed 880m/min	0 ACH
19	1.10	1.04	0	0.05	1.26	1.07	0.01	0.05	Sawing	MWCNT	Sawing speed 410m/min	0 ACH
20	1.12	1.03	0.01	0.06	1.30	1.06	0.01	0.05	Sawing	MWCNT	Sawing speed 410m/min	0 ACH
21	1.12	1.04	0.02	0.05	1.28	1.05	0.01	0.05	Sawing	MWCNT	Sawing speed 410m/min	0 ACH

22	1.05	1.03	-0.03	0.06	1.16	1.07	-0.03	0.06	Sawing	MWCNT	Sawing speed 880m/min	3.5 ACH
23	1.16	1.06	0.07	0.06	1.33	1.08	0.07	0.06	Sawing	MWCNT	Sawing speed 880m/min	3.5 ACH
24	1.07	1.06	0	0.05	1.17	1.09	-0.05	0.06	Sawing	MWCNT	Sawing speed 880m/min	3.5 ACH
25	1.14	1.05	-0.03	0.06	1.27	1.04	-0.07	0.06	Sawing	OP	Sawing speed 410m/min	3.5 ACH
26	1.04	1.05	-0.15	0.05	1.15	1.05	-0.14	0.06	Sawing	OP	Sawing speed 410m/min	3.5 ACH
27	1.09	1.04	-0.1	0.05	1.27	1.09	-0.04	0.05	Sawing	OP	Sawing speed 410m/min	3.5 ACH
28	1.01	1.03	-0.05	0.05	1.07	1.05	-0.03	0.06	Sawing	OP	Sawing speed 880m/min	0 ACH
29	0.97	1.04	-0.12	0.07	1.11	1.08	-0.14	0.08	Sawing	OP	Sawing speed 880m/min	0 ACH
30	1.00	1.05	-0.05	0.06	1.12	1.07	-0.02	0.06	Sawing	OP	Sawing speed 880m/min	0 ACH
31	0.99	1.04	-0.09	0.05	1.14	1.07	-0.07	0.06	Sawing	OP	Sawing speed 410m/min	0 ACH
32	0.93	1.06	-0.15	0.06	1.16	1.12	-0.08	0.06	Sawing	OP	Sawing speed 410m/min	0 ACH
33	0.95	1.05	-0.1	0.05	1.06	1.09	-0.12	0.07	Sawing	OP	Sawing speed 410m/min	0 ACH
34	1.06	1.05	-0.02	0.06	1.21	1.08	-0.08	0.06	Sawing	OP	Sawing speed 880m/min	3.5 ACH
35	0.98	1.04	-0.1	0.05	1.10	1.06	-0.17	0.05	Sawing	OP	Sawing speed 880m/min	3.5 ACH
36	1.03	1.07	0.01	0.05	1.13	1.12	-0.17	0.07	Sawing	OP	Sawing speed 880m/min	3.5 ACH

GM: Geometric mean, GSD: Geometric standard deviation, NF: near field, FF: far field, OP: organic pigment, MWCNT: multi-walled carbon nanotubes, ACH: air change per hour

Table S4: Original results per experiment (GM and GSD) of the particle size and results of the first stage analyses for ELPI estimated β and SE (log-transformed) of the activity-effect level (background corrected) and determinants.

	Activity-effect level NF				**Activity-effect level FF**				**Exposure determinants**			
Exp. No.	**GM**	**GSD**	**Mean**	**Standard error**	**GM**	**GSD**	**Mean**	**Standard error**	**Activity**	**Car bumper**	**Settings machine**	**Mechanical**

	(nm)		(β)	(SE)	(nm)		(β)	(SE)				ventilation
1	10.93	1.02	0	0.01	46.22	1.31	-0.03	0.02	Drilling	MWCNT	Drill size 4 mm	0 ACH
2	10.82	1.01	0.01	0.01	50.66	1.41	0.05	0.02	Drilling	MWCNT	Drill size 4 mm	0 ACH
3	11	1.10	-0.01	0.01	46.01	1.33	-0.04	0.02	Drilling	MWCNT	Drill size 4 mm	0 ACH
4	12.12	1.16	0.05	0.01	43.96	1.22	-0.27	0.02	Drilling	MWCNT	Drill size 8mm	0 ACH
5	11.95	1.06	0.03	0.000001	55.91	1.22	-0.02	0.02	Drilling	MWCNT	Drill size 8mm	0 ACH
6	12.15	1.09	0.05	0.01	42.84	1.16	-0.29	0.01	Drilling	MWCNT	Drill size 8mm	0 ACH
7	13.14	1.08	0.02	0.01	54.87	1.09	-0.04	0.01	Drilling	OP	Drill size 4 mm	0 ACH
8	12.78	1.09	-0.01	0.01	54.67	1.09	-0.05	0.01	Drilling	OP	Drill size 4 mm	0 ACH
9	15.63	1.29	0.19	0.01	57.33	1.08	-1E-06	0.01	Drilling	OP	Drill size 4 mm	0 ACH
10	-	-	-	-	33.48	1.06	-0.11	0.01	Drilling	OP	Drill size 8mm	0 ACH
11	-	-	-	-	50.95	1.10	0.31	0.01	Drilling	OP	Drill size 8mm	0 ACH
12	-	-	-	-	44.96	1.09	0.19	0.01	Drilling	OP	Drill size 8mm	0 ACH
13	10.68	1.04	0.08	0.01	50.91	1.19	0.01	0.01	Sawing	MWCNT	Sawing speed 410m/min	3.5 ACH
14	27.22	3.10	1.02	0.07	59.64	1.19	0.17	0.01	Sawing	MWCNT	Sawing speed 410m/min	3.5 ACH
15	10.09	1.02	0.02	0.000001	51.04	1.23	0.02	0.01	Sawing	MWCNT	Sawing speed 410m/min	3.5 ACH
16	10.52	1.04	0.05	0.000001	58.16	1.29	0.62	0.01	Sawing	MWCNT	Sawing speed 880m/min	0 ACH
17	10.66	1.05	0.06	0.000001	64.48	1.33	0.73	0.01	Sawing	MWCNT	Sawing speed 880m/min	0 ACH
18	13.55	1.60	0.29	0.03	46.47	1.30	0.4	0.01	Sawing	MWCNT	Sawing speed 880m/min	0 ACH

19	12.84	1.07	0.21	0.01	51.63	1.16	0.14	0.01	Sawing	MWCNT	Sawing speed 410m/min	0 ACH
20	17.91	1.26	0.54	0.02	56.18	1.07	0.22	0.01	Sawing	MWCNT	Sawing speed 410m/min	0 ACH
21	17.30	1.17	0.51	0.01	58.06	1.05	0.25	0.01	Sawing	MWCNT	Sawing speed 410m/min	0 ACH
22	21.81	1.28	0.72	0.01	56.31	1.20	0.46	0.01	Sawing	MWCNT	Sawing speed 880m/min	3.5 ACH
23	19.59	1.40	0.62	0.02	77.41	1.28	0.77	0.01	Sawing	MWCNT	Sawing speed 880m/min	3.5 ACH
24	21.59	1.37	0.72	0.02	73.55	1.24	0.72	0.01	Sawing	MWCNT	Sawing speed 880m/min	3.5 ACH
25	17.50	1.41	0.46	0.02	48.18	1.25	0.11	0.02	Sawing	OP	Sawing speed 410m/min	3.5 ACH
26	-	-	-	-	41.37	1.10	-0.05	0.01	Sawing	OP	Sawing speed 410m/min	3.5 ACH
27	15.41	1.23	0.07	0.01	44.54	1.18	0.03	0.01	Sawing	OP	Sawing speed 410m/min	3.5 ACH
28	11.95	1.02	0.05	0.01	49.22	1.19	0.46	0.01	Sawing	OP	Sawing speed 880m/min	0 ACH
29	10.62	10.07	0.01	0.00001	48.70	1.17	0.45	0.01	Sawing	OP	Sawing speed 880m/min	0 ACH
30	10.22	1.04	0.06	0.00001	35.83	1.11	0.15	0.01	Sawing	OP	Sawing speed 880m/min	0 ACH
31	10.21	1.02	0.07	0.01	45.17	1.17	-0.05	0.01	Sawing	OP	Sawing speed 410m/min	0 ACH
32	10.39	1.08	0.08	0.01	45.48	1.22	-0.04	0.02	Sawing	OP	Sawing speed 410m/min	0 ACH
33	10.49	1.03	0.11	0.00001	47.80	1.17	0.01	0.01	Sawing	OP	Sawing speed 410m/min	0 ACH
34	11.12	1.05	0.08	0.01	59.46	1.13	0.61	0.01	Sawing	OP	Sawing speed 880m/min	3.5 ACH
35	10.74	1.06	0.16	0.01	57.67	1.20	0.58	0.01	Sawing	OP	Sawing speed 880m/min	3.5 ACH
36	11.74	1.19	0.08	0.01	49.01	1.18	0.41	0.01	Sawing	OP	Sawing speed 880m/min	3.5 ACH

GM: Geometric mean, GSD: Geometric standard deviation, NF: near field, FF: far field, OP: organic pigment, MWCNT: multi-walled carbon nanotubes, ACH: air change per hour